Electronic Supplementary Material (ESI) for Journal of Materials Chemistry C.

Electronic Supporting Information

High-Efficiency Solution-Processed OLEDs Based on Cationic Ag_6Cu Heteroheptanuclear Cluster Complexes with Aromatic Acetylides

Liang-Jin Xu, Xu Zhang, Jin-Yun Wang, and Zhong-Ning Chen*

State Key Laboratory of Structural Chemistry, Fujian Institute of Research on the Structure of Matter, Chinese Academy of Sciences, Fuzhou, Fujian 350002, China

Table S1. Selected Atomic Distances (Å) and Angles (°) of **1**·6CH$_2$Cl$_2$ and **4**·3CH$_2$Cl$_2$.

1·6CH$_2$Cl$_2$

Ag1–Cu1	2.6586(10)	Ag2–Cu1	2.6312(10)
Ag3–Cu1	2.7099(11)	Ag4–Cu1	2.8146(11)
Ag5–Cu1	2.8087(10)	Ag6–Cu1	2.6803(10)
Ag1–C135	2.472(8)	Ag1–C123	2.649(7)
Ag1–P1	2.4110(19)	Ag1–O5	2.287(5)
Ag2–C111	2.493(7)	Ag2–C135	2.658(7)
Ag2–P2	2.407(2)	Ag2–O1	2.248(6)
Ag3–C123	2.470(8)	Ag3–O3	2.253(5)
Ag3–P3	2.424(2)	Ag4–P4	2.4189(19)
Ag4–C111	2.415(7)	Ag4–O2	2.253(6)
Ag5–C135	2.285(7)	Ag5–O6	2.285(6)
Ag5–P5	2.396(2)	Ag6–P6	2.3987(19)
Ag6–C123	2.364(7)	Ag6–O4	2.210(5)
Cu1–C111	1.944(7)	Cu1–C123	1.959(7)
Cu1–C135	1.977(7)	Ag1–Cu1–Ag2	78.80(3)
Ag1–Cu1–Ag3	80.77(3)	Ag2–Cu1–Ag3	78.87(3)
Ag4–Cu1–Ag5	74.25(3)	Ag4–Cu1–Ag6	81.99(3)
Ag5–Cu1–Ag6	85.02(3)	Ag2-Cu1-Ag6	147.82(4)
Ag1-Cu1-Ag6	125.51(4)	C111–Cu1–C123	122.4(3)
C111–Cu1–C135	116.7(3)	C123–Cu1–C135	120.1(3)

5·3CH$_2$Cl$_2$

Ag1–Cu1	2.6722(10)	Ag2–Cu1	2.7856(10)
Ag1–P1	2.4246(15)	Ag2–P2	2.3795(15)
Ag2–C39	2.265(6)	Ag2–S2A	2.281(5)
Ag1–S1	2.250(4)	Cu1–C39	1.957(5)
Ag1–Cu1–Ag1A	81.54(4)	Ag2–Cu1–Ag1B	148.066(13)
Ag1–Cu1–Ag2	124.958(13)	C39–Cu1–C39B	119.89(2)
C39–Cu1–C39A	119.89(2)	C39A–Cu1–C39B	119.89(2)

Table S2. The Partial Molecular Orbital Compositions (%) and the Absorptions Transitions for Complex **1** in CH_2Cl_2 Media Calculated by TD-DFT method at the PBE1PBE level.

orbital	energy	MO contribution (%)				
	(eV)	Cu (s/p/d)	Ag (s/p/d)	$HC(PPh_2)_3$	Ph_2PO_2	$C{\equiv}CC_6H_4Bu^t$-4
LUMO+4	-1.23	26.32 (0/97/3)	21.60 (52/45/3)	19.17	1.57	31.35
LUMO+3	-1.23	27.20 (0/98/2)	21.41 (52/45/3)	19.75	1.59	30.06
LUMO	-2.28	34.68 (0/100/0)	31.50 (75/13/12)	12.16	0.26	21.39
HOMO	-6.31	8.56 (0/20/80)	19.75 (8/21/70)	10.53	1.13	60.03
HOMO-1	-6.32	8.26 (0/21/79)	19.81 (7/21/72)	11.18	1.01	59.74
HOMO-3	-6.66	24.45 (0/29/71)	24.48 (5/16/79)	12.59	6.15	32.33
HOMO-4	-6.66	20.64 (0/30/70)	26.71 (5/16/79)	16.68	7.36	28.61
HOMO-7	-6.90	8.87 (5/7/87)	20.16 (11/20/69)	54.40	7.94	8.63
HOMO-9	-7.00	7.55 (0/51/49)	36.29 (17/16/67)	36.23	12.56	7.37
HOMO-11	-7.13	11.41 (1/99/0)	17.91 (41/16/43)	34.45	19.24	16.99
HOMO-14	-7.22	24.73 (7/92/0)	22.18 (59/11/30)	30.39	14.88	7.82

state	*E*, nm (eV)	O.S.	component	CI coef.	assignment	measured (nm)
S_1	389 (3.19)	0.1006	HOMO→LUMO	39%	^{1}LMCT/^{1}MC^1/IL	
			HOMO-1→LUMO	30%	^{1}LMCT/^{1}MC^1/IL	
			HOMO-4→LUMO	20%	^{1}MC/^{1}IL/^{1}LMCT	
S_2	388 (3.20)	0.1011	HOMO-1→LUMO	35%	^{1}LMCT/^{1}IL/^{1}MC	
			HOMO→LUMO	30%	^{1}LMCT/^{1}IL/^{1}MC	
			HOMO-3→LUMO	26%	^{1}MC/^{1}IL/^{1}LMCT	
S_4	361 (3.44)	0.156	HOMO-3→LUMO	57%	^{1}MC/^{1}IL/^{1}LMCT	364
			HOMO-1→LUMO	26%	^{1}LMCT/^{1}IL/^{1}MC	
S_5	358 (3.46)	0.1389	HOMO-4→LUMO	59%	^{1}MC/^{1}IL/^{1}LMCT	
			HOMO→LUMO	21%	^{1}LMCT/^{1}IL/^{1}MC	
S_8	324 (3.83)	0.1145	HOMO-7→LUMO	67%	^{1}LMCT/^{1}MC/^{1}IL/^{1}LLCT	
S_{10}	315 (3.94)	0.1558	HOMO-9→LUMO	89%	^{1}MC/^{1}LMCT/^{1}IL/^{1}LLCT	
S_{11}	307 (4.03)	0.2712	HOMO-11→LUMO	31%	^{1}LMCT/^{1}MC/^{1}IL	305
			HOMO-7→LUMO	21%	^{1}LMCT/^{1}MC/^{1}IL/^{1}LLCT	
			HOMO-14→LUMO	13%	^{1}MC/^{1}LMCT/^{1}LLCT	
S_{24}	283 (4.39)	0.3762	HOMO-1→LUMO+3	25%	^{1}IL/^{1}MC/^{1}LMCT/^{1}LLCT	275
			HOMO→LUMO+4	15%	^{1}IL/^{1}MC/^{1}LMCT/^{1}LLCT	

Table S3. The Partial Molecular Orbital Compositions (%) and the Emission Transitions for Complex **1** in CH_2Cl_2 Media, Calculated by TD-DFT method at the PBE1PBE level.

orbital	energy (eV)	MO contribution (%)				
		Cu (s/p/d)	Ag (s/p/d)	$HC(PPh_2)_3$	Ph_2PO_2	$C{\equiv}CC_6H_4Bu^t$-4
LUMO+3	-1.33	29.18 (0/97/3)	22.73 (51/46/3)	12.03	1.41	34.64
LUMO	-2.61	37.82 (1/99/0)	36.58 (84/8/8)	8.90	0.26	16.45
HOMO	-6.06	11.31 (3/32/65)	16.08 (17/23/60)	5.93	1.63	65.05

state	*E*, nm (eV)	O.S.	component	CI coef.	assignment	measured (nm)
T_1	574 (2.16)	0.0000	HOMO→LUMO	73%	^{3}LMCT/^{3}MC	575
			HOMO→LUMO+3	16%	^{3}IL/^{3}MC/^{3}LMCT	

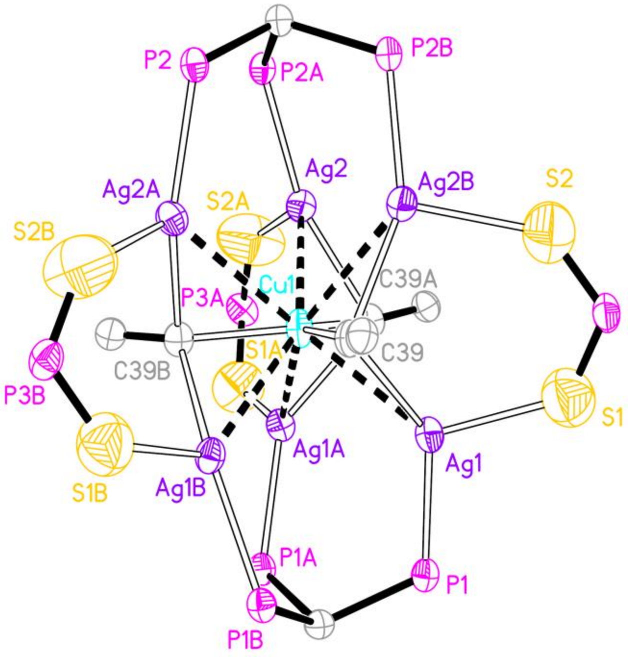

Figure S1. ORTEP drawings of the complex cation of **5** with atom labeling scheme showing 30% thermal ellipsoids. Phenyl rings on the phosphorus atoms and acetylides are omitted for clarity.

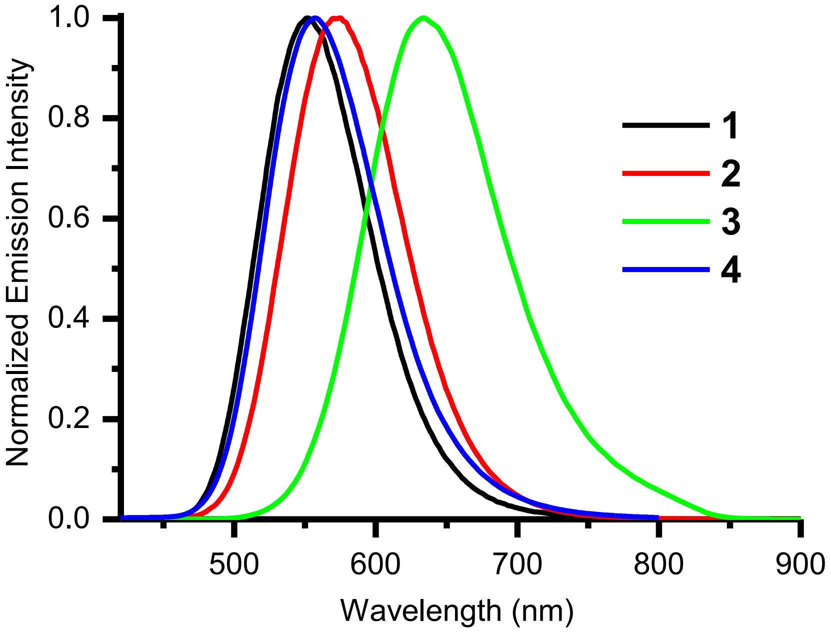

Figure S2. Emission spectra of complexes **1**–**4** in desolvate powders at ambient temperature.

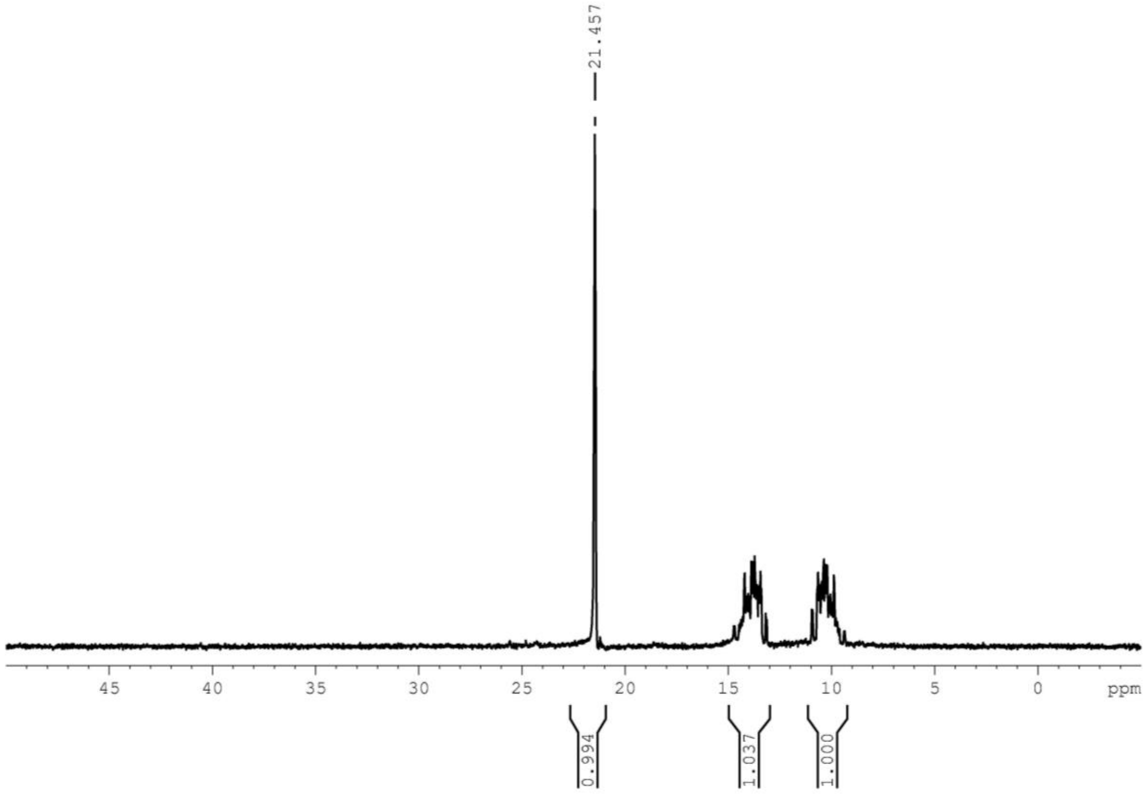

Figure S3. The ^{31}P NMR spectrum of complex **1** in CD_2Cl_2.

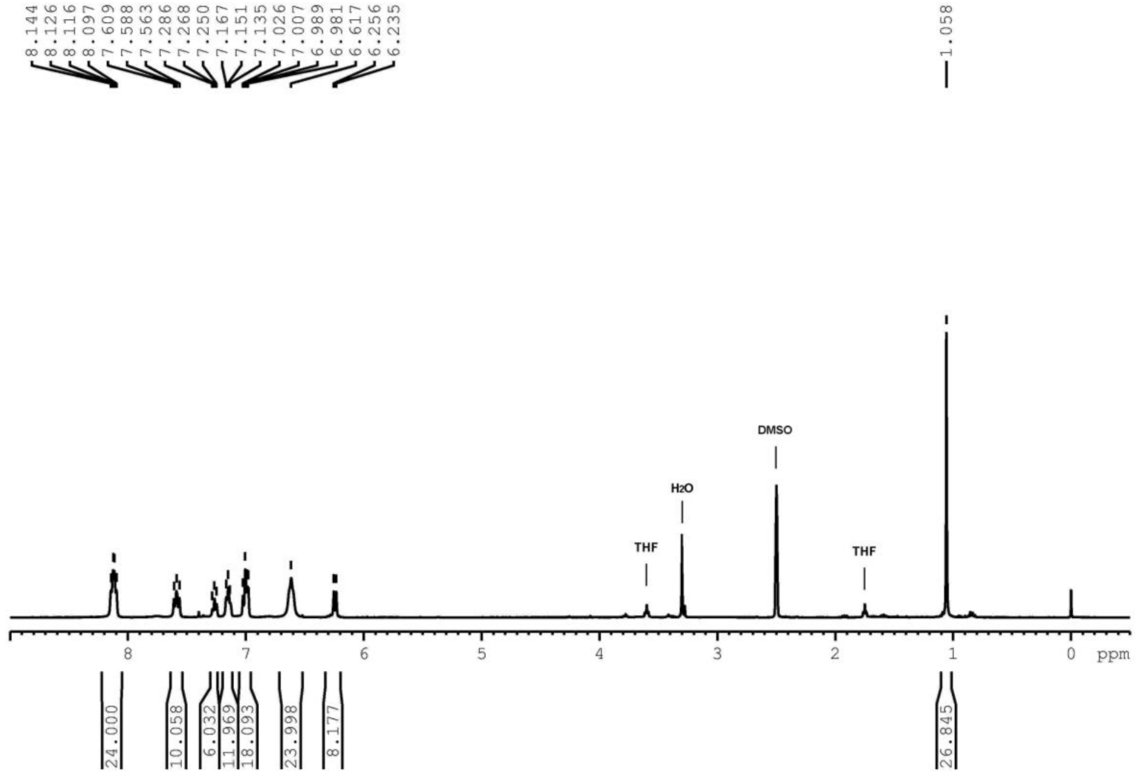

Figure S4. ^{1}H NMR spectrum of complex **1** upon exposure to THF vapor, measured in DMSO-d_6.

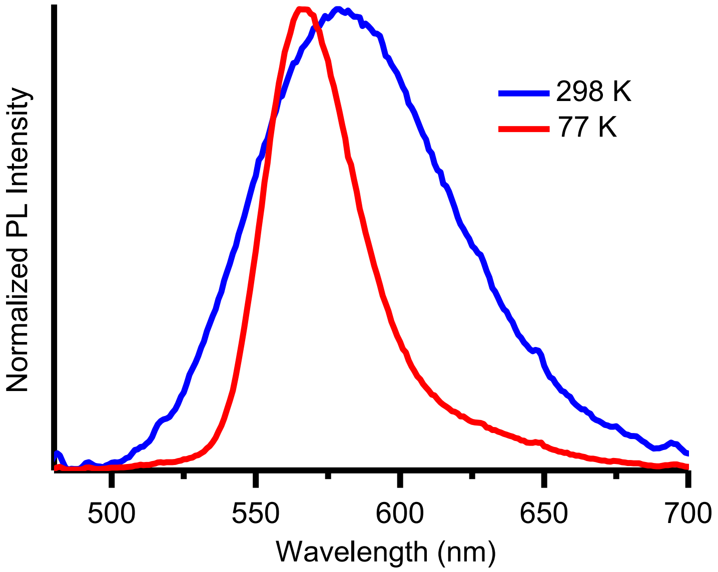

Figure S5. The emission spectra of complex **1** in fluid CH_2Cl_2 at 298 K and frozen glass at 77 K.

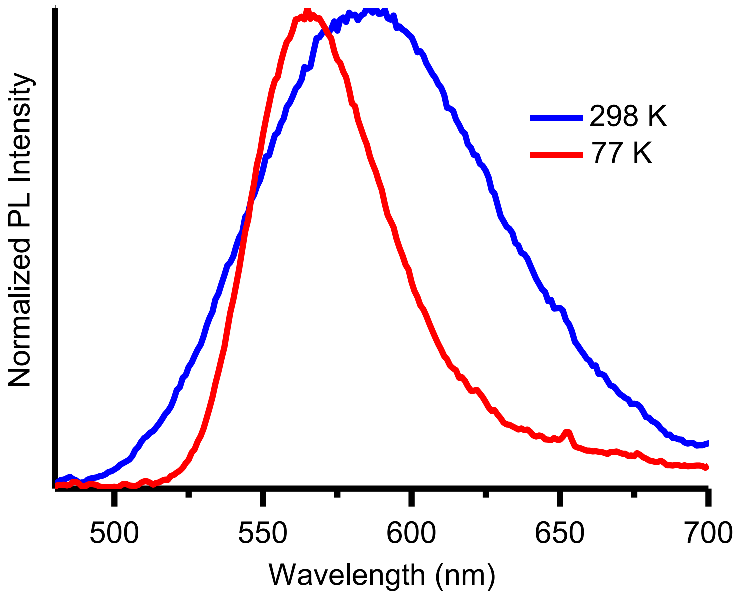

Figure S6. The emission spectra of complex **4** in fluid CH_2Cl_2 at 298 K and frozen glass at 77 K.

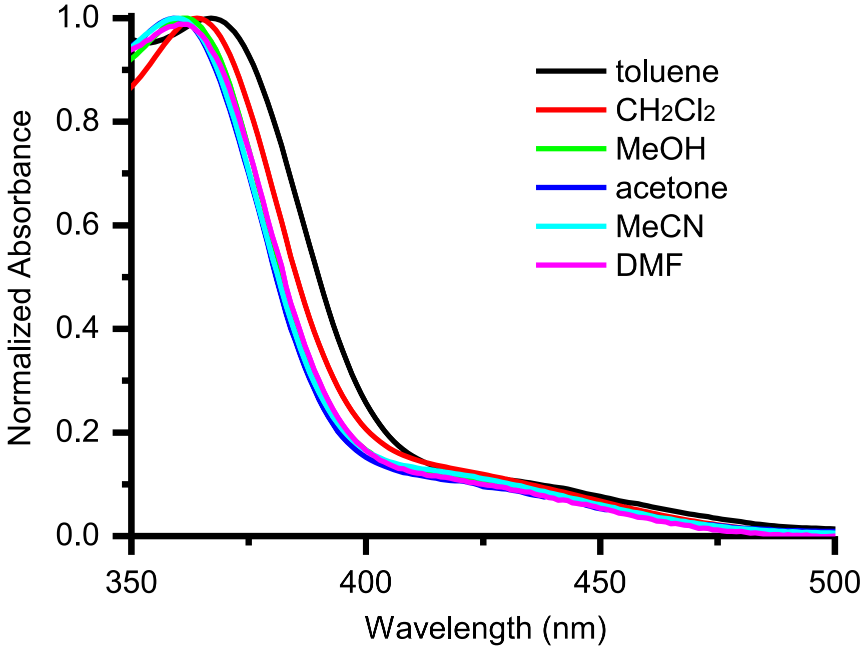

Figure S7. The UV-Vis absorption spectra of complex **1** in various solutions at ambient temperature.

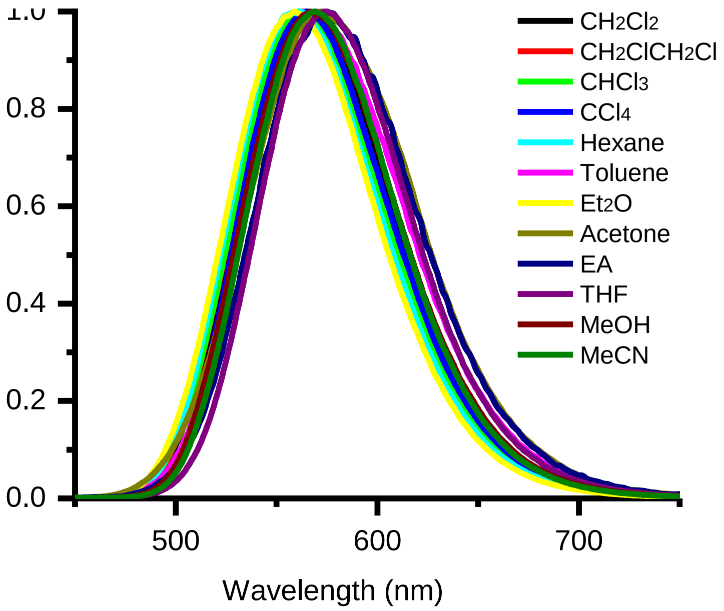

Figure S8. Emission spectra of **2** in the solid state upon exposure to various VOC vapors at ambient temperature.

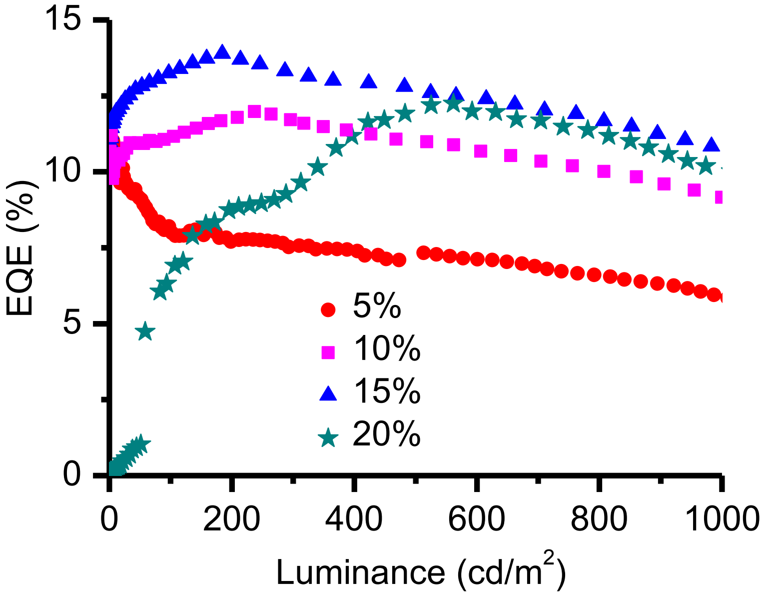

Figure S9. External quantum efficiency *vs* luminance of the devices with different doping percentage of complex **4** in the emitting layer with weight ratio of mixed host TCTA : OXD-7 being in 2 : 1.

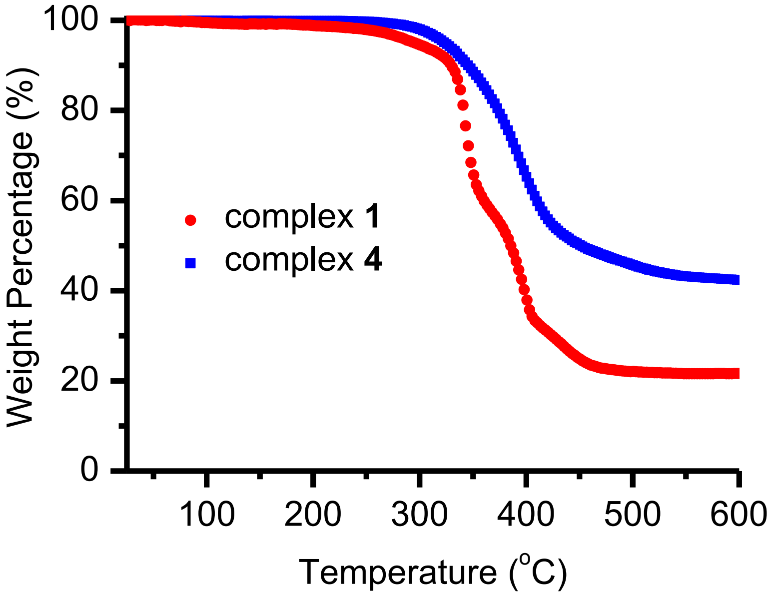

Figure S10. Plots of thermogravimetric analysis for desolvated complexes **1** and **4** at temperature range 25–600 °C.

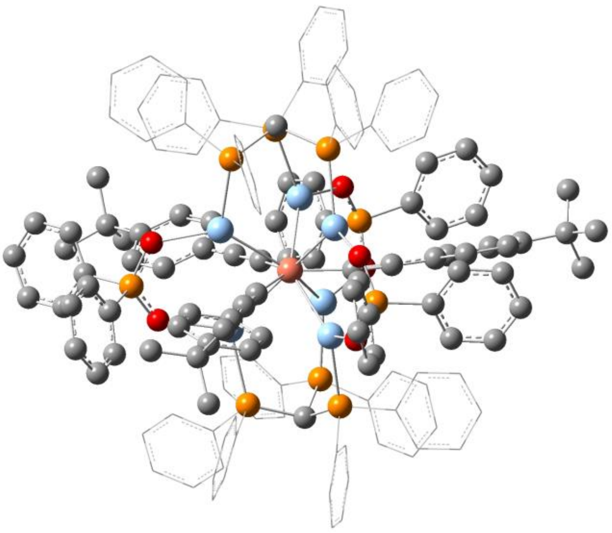	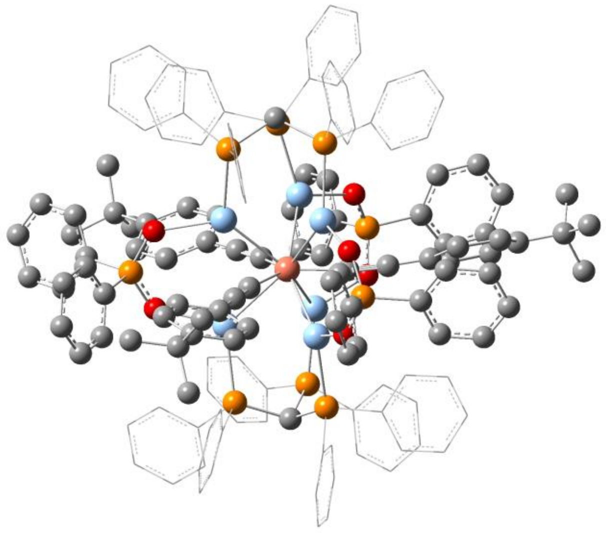
S_0	T_1

Figure S11. The optimized geometrical structures of complex **1** in ground state and lowest-energy triplet state by DFT method at the PBE1PBE level. For clarity, the hydrogen atoms are omitted and phenyl rings in the $HC(PPh_2)_3$ are in the wireframe model.

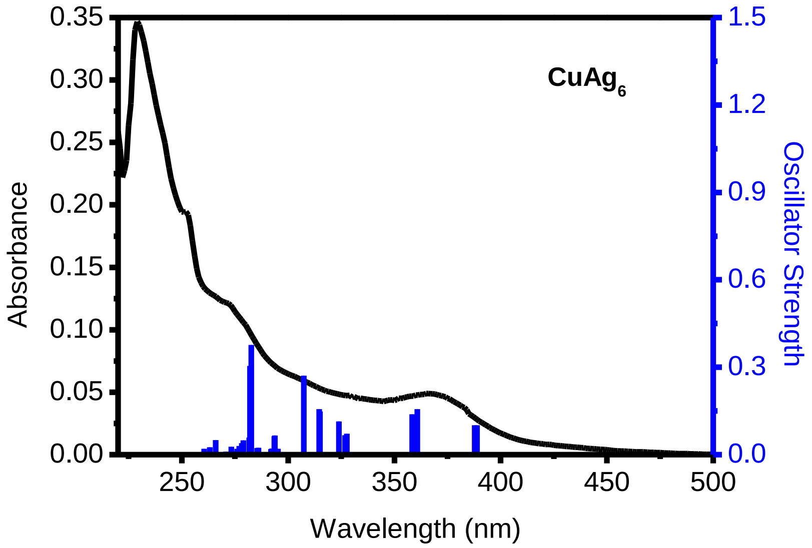

Figure S12. The calculated (blue vertical bars) and measured (black line) UV/Vis absorption spectra of complex **1** in dichloromethane at ambient temperature calculated by TD-DFT method at the PBE1PBE level.

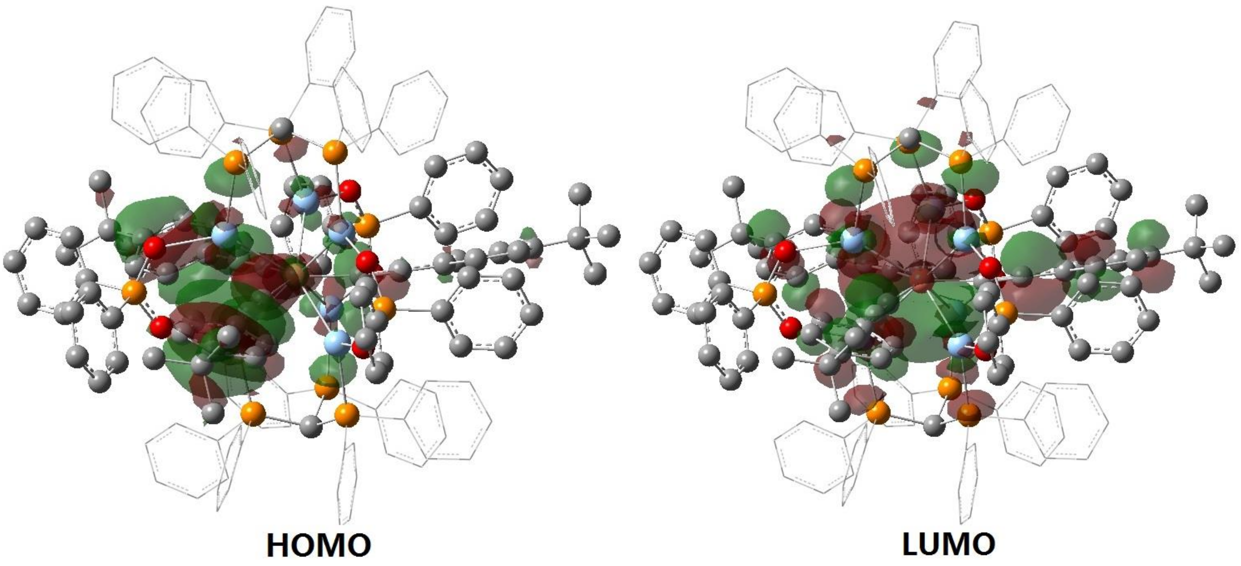

HOMO LUMO

Figure S13. Plots of the frontier molecular orbitals involved in the absorption transitions for complex **1** in dichloromethane solution calculated by TD-DFT method at the PBE1PBE level (isovalue = 0.02). For clarity, the hydrogen atoms are omitted and the phenyl rings in $HC(PPh_2)_3$ are in the wireframe model.

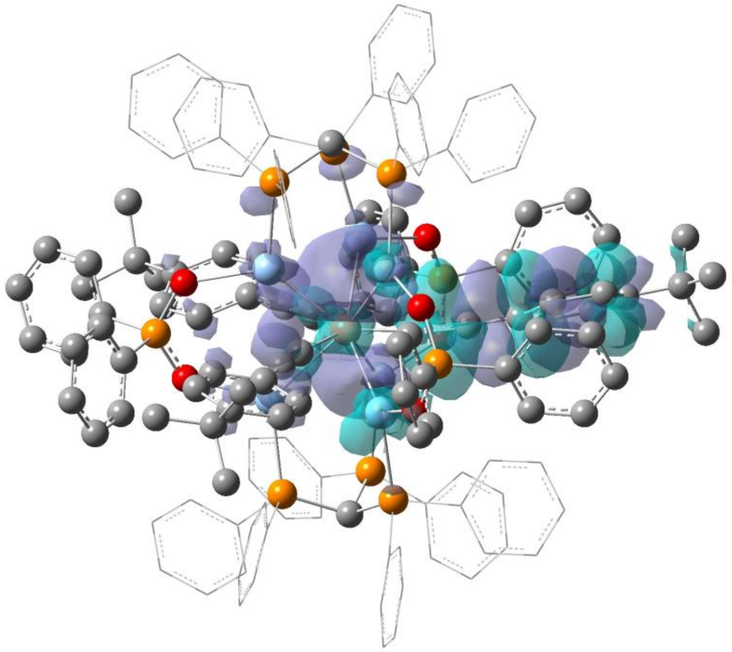

Figure S14. Plots of electron density difference (EDD) of $\Delta\rho(T_1\text{-}S_0)$ between the first triplet excited state (T_1) and ground state (S_0) for complex **1** in dichloromethane, calculated by TD-DFT method at the PBE1PBE level (isovalue = 0.0004). The green colors represent the electron depletion (ED) region, while the purple ones suggest the electron accumulation (EA) region. For clarity, the hydrogen atoms are omitted and phenyl rings in $HC(PPh_2)_3$ are in the wireframe model.